

Differential Regulation of *Slc40a1*, *Fth1*, and *Hmox1* by Deferasirox in Splenic Iron Overload

Annisa Maharani Wibowo, Yasmi Purnamasari Kuntana, Tanendri Arrizqiani, Ratu Safitri ✉

[The author informations are in the declarations section. This article is published by ETFLIN in Sciences of Pharmacy, Volume 4, Issue 4, 2025, Page 286-291. DOI 10.58920/sciphar0404386]

Received: 24 June 2025

Revised: 31 July 2025

Accepted: 06 August 2025

Published: 10 November 2025

Editor: Pilli Govindaiah

This article is licensed under a Creative Commons Attribution 4.0 International License. © The author(s) (2025).

Keywords: Deferasirox therapy, Iron overload, Splenic gene expression, *Fth1*, *Slc40a1*, *Hmox1*.

Abstract: Iron overload, often arising from repeated transfusions in thalassemia major, disrupts iron homeostasis and induces oxidative stress. Deferasirox is a widely used oral chelator, yet its effects on splenic iron-regulatory gene expression remain unclear. This study investigated the impact of deferasirox on ferritin heavy chain (*Fth1*), ferroportin (*Slc40a1*), and heme oxygenase-1 (*Hmox1*) expression in a rat model of splenic iron overload. Eighteen male Wistar rats were randomly assigned into three groups ($n = 6$ each): normal (N), iron dextran-induced overload without treatment (KN), and iron overload treated with deferasirox (KP). Gene expression was quantified by real-time PCR using the $2^{-\Delta\Delta CT}$ (Livak) method, with statistical analysis performed via one-way ANOVA and Tukey's post hoc test. Iron overload significantly upregulated *Fth1* (2.26-fold) and *Slc40a1* (1.72-fold) versus controls ($p < 0.05$). Deferasirox treatment reduced *Fth1* (3.28-fold decrease) and *Slc40a1* (1.15-fold reduction) relative to untreated overload, though not significantly ($p > 0.05$). In contrast, *Hmox1* expression markedly increased (55.25-fold, $p < 0.05$) following deferasirox administration. These results indicate that deferasirox selectively modulates splenic iron-regulatory genes, suggesting both chelation and adaptive stress-response mechanisms, thereby supporting its therapeutic role in managing iron overload.

Introduction

Iron overload is a condition that develops when the body has an abnormally high accumulation of iron, resulting from either dietary intake or repeated blood transfusions. This condition can be fatal due to the reactive nature of free iron, which promotes the formation of free radicals, specifically hydroxyl radicals (1). The accumulation of these free radicals triggers oxidative stress, which, if left unaddressed, ultimately leads to tissue and organ damage (2). Iron overload from regular blood transfusions is a significant cause of morbidity and mortality in patients with thalassemia major (3). Various complications have been observed in patients with iron overload due to repeated transfusions, including endocrine dysfunction, hypogonadism, hypothyroidism, cardiomyopathy, arrhythmias, renal abnormalities, and even renal failure. These complications typically manifest in pediatric and adult patients with an average age of 31.3 years, following a transfusion duration of 12-18 years (4).

Excessive iron accumulation significantly impacts various organs, particularly those involved in iron regulation, with the spleen being a notable example (5). The spleen, a reddish-black organ located in the cranial left abdomen, is vital for maintaining physiological stability through diverse roles, including initiating immune responses in the blood and maintaining iron homeostasis by breaking down heme in

aged red blood cells into biliverdin, carbon monoxide, and ferrous iron, mediated by the *Hmox1* enzyme (6, 7). Splenic iron overload can be assessed by examining the levels of iron homeostasis-regulating proteins, including ferritin, hepcidin, ferroportin, HRG1, and heme oxygenase. Among these, ferritin, ferroportin, and heme-oxygenase are three key proteins encoded by the genes Ferritin heavy chain (*Fth1*), solute carrier family 40 member 1 (*Slc40a1*), and heme oxygenase 1 (*Hmox1*), respectively. These proteins play crucial roles in iron storage, transport, and the breakdown of erythrocyte iron that is catabolized in the spleen (8). *Fth1* serves as a critical component for the oxidation of ferrous iron and its subsequent transfer to the ferritin core for storage (9). This makes it a primary biomarker for iron overload, characterized by increased *Fth1* expression (10). As the sole iron export pathway in mammals, *Slc40a1* expression is reported to increase in conditions of iron overload to prevent iron accumulation in affected tissues (11). Consistent with the trends of the other two genes, *Hmox1* shows upregulation of expression when body iron levels rise (12). These findings indicate a mechanism of resistance to iron overload, in addition to its primary function as a heme-degrading enzyme (13). Given the lack of a distinct iron removal mechanism, iron chelating agents are crucial for mitigating excessive iron accumulation within the body, thereby preventing oxidative stress (14).

Currently, deferiprone, deferoxamine, and deferasirox are the primary iron-chelating agents used in clinical practice. Each of these chelators possesses distinct dosages, mechanisms of action, and advantages (15). Among them, deferasirox represents the newest chelating agent, demonstrating superior iron-chelating efficacy and a lower side effect profile, albeit at a relatively higher cost (16). Deferasirox is an oral medication for iron overload that works by binding to iron in a 2:1 ratio. The primary indicator for Deferasirox administration is a serum ferritin level of 1000 ng/mL or higher (17). Emerging evidence suggests that deferasirox contributes to the maintenance of iron homeostasis by modulating key iron-regulatory genes, including *HAMP*, *Pu1*, *Gata1*, and *Gdf11* (18).

Previous research has extensively demonstrated the effectiveness of deferasirox in reducing systemic iron levels. However, its influence on the gene expression of *Slc40a1*, *Fth1*, and *Hmox1* has yet to be investigated. Considering this knowledge gap, the present study aims to isolate these genes (*Slc40a1*, *Fth1*, and *Hmox1*) from the spleens of iron-overloaded rat models, following treatment with the chelating agent deferasirox, to evaluate the impact of this chelator on their expression levels.

Experimental Section

Materials

The following materials were utilized in this study: 18 Wistar strain white rats (*Rattus norvegicus*) weighing 150-200 mg obtained from Biofarma, Indonesia. Rats were injected with Hemadex® iron dextran (Sanbe, Indonesia) combined with 0,9% sodium chloride (Otsuka, Indonesia) to induce an iron overload condition and then treated with Deferasirox (KalbeMed, Indonesia). Ket-A-Xyl® (Agrovet, Spain) has been used to anesthetize rats. The kit for RNA isolation includes the FIREScript RT cDNA Synthesis Kit (Solis BioDyne, Estonia), the Quick-RNA™ Miniprep Plus Kit (Zymo Research, USA), and the HOT FIREPol® EvaGreen® qPCR Mix Plus (Solis BioDyne, Estonia). Other materials used in this study include alcohol 70% (OneMed, Indonesia), absolute ethanol (Merck, Germany), distilled water (Cleo, Indonesia), and liquid nitrogen. The equipment used in this research included: Disposable Syringes (OneMed, Indonesia), surgical trays, dissecting set (OneMed, Indonesia), PCR Tube 0,2 mL (OneMed, Indonesia), Adjustable Micropipettes (Dragonlab, China), Disposable Tissue Grinder (Axyste, China), centrifuge (Thermo Fisher, USA), vortex mixer (Thermo Fisher, USA), Rapi:chip™ 10-well PCR Chip Standard Pack (Genesystem, Korea), and a Real-Time Polymerase Chain Reaction (RT-PCR) Genechecker UF-300 system (Genesystem, Korea).

In Vivo Test

Animal Preparation

This study utilized 18 Wistar strain white rats (*Rattus norvegicus*) based on Mead's Resource Equation Method (19). Sample size was estimated using Mead's Resource Equation, which is appropriate for exploratory animal studies with limited prior data. Additionally, based on a power analysis using G*Power software, a minimum of 6 animals per group was required to detect a medium effect size ($f = 0.40$) with 80% power at an α level of 0.05. Therefore, a total of 18 animals ($n = 6$ per group) was deemed adequate for statistical analysis and biological relevance. The animals were randomly divided into three treatment groups, with six rats in each: a normal control group (N), an iron dextran

group (KN), and an iron dextran + deferasirox group (KP). All procedures involving animal subjects in this study received ethical approval from the Ethics Committee of Universitas Padjadjaran (Code: 75/UN6.KEP/EC/2023). Animal handling was performed with the utmost care, adhering to OECD animal welfare guidelines to minimize distress throughout the study. Before administration, Wistar rats were acclimatized for 7 days. During the acclimatization period, the rats were provided with standardized, iron-free nutritional food from ARIC UNPAD and given iron-free water *ad libitum* to prevent dietary iron overload. Body weights were measured every 3 days to ensure weight maintenance. Cage bedding was changed every 3 days. The animals were maintained under a 12-hour light/12-hour dark cycle (20).

Iron Dextran and Deferasirox Administration

Iron dextran was administered at a dose of 120 mg/kg body weight, as adapted from (21). We hypothesize that the administered dose will effectively double the iron levels in the rats' bodies compared to the previously established baseline. Iron dextran was administered intravenously to three experimental groups (KN and KP) every 3 days for a total duration of 15 days. The daily iron dextran dose was 10 mg/kg body weight. For a rat weighing 200 g, this daily dose was converted to 2.4 mg/rat/day.

Representing the optimal human equivalent dose, the animals received a 30 mg/kg dose of deferasirox (22). Administration was performed daily at 08:00 AM to the experimental groups KP for 28 days. The selected dose and 14-day treatment duration were based on previous studies demonstrating both efficacy and safety in rodent models of iron overload (23). This duration was also sufficient to assess changes in gene expression in response to chelation therapy. Before administration, the deferasirox dose was converted for a 200 g rat by multiplying it by a conversion factor of 0.018 (24). According to this conversion, the administered dose was 0.189 mg/g body weight of the rat.

Spleen Organ Collection

Before sacrifice, each experimental rat model was fasted for 16 h following the last treatment. Rats were anesthetized intramuscularly with ketamine-xylazine and placed on a dissecting board. Dissection commenced from the abdominal region, extending to the chest using surgical scissors. Subsequently, the spleen organ was carefully removed and immediately placed into a cryotube, which was then stored in a -20 °C freezer.

RNA Isolation and Purification

Total RNA was isolated from homogenized organ samples using the Quick-RNA Miniprep Plus Kit (Zymo Research) according to the manufacturer's instructions. Briefly, 300 μ L of homogenized sample, mixed with DNA/RNA Shield™, was incubated with Proteinase K and PK Digestion Buffer for 30 min at room temperature (20–30 °C). After debris removal by centrifugation, the supernatant was mixed with an equal volume of RNA Lysis Buffer. RNA purification involved transferring the lysed sample to a Spin-Away™ Filter and centrifuging. Ethanol was added to the flow-through, and the mixture was loaded onto a Zymo-Spin™ IIICG Column and centrifuged. The column underwent washes with RNA Wash Buffer. On-column DNase treatment was performed using DNase I and DNA Digestion Buffer for 15 min at room temperature. The column was then sequentially washed with

RNA Prep Buffer and RNA Wash Buffer. Finally, the RNA was eluted with DNase- and RNase-free water. RNA purity was confirmed by spectrophotometry (Nanodrop), with A260/A280 ratios between 1.8 and 2.0 considered acceptable. Purified RNA was stored at 4 °C.

DNA Synthesis

Complementary DNA (cDNA) synthesis was performed using the Takara Bio cDNA Kit, following a multi-step protocol. The first-strand cDNA synthesis was initiated by preparing a reaction mixture according to the kit's instructions. Subsequently, for second-strand cDNA synthesis and conversion of the RNA template to DNA, additional components were added to the 20 µL first-strand cDNA synthesis mixture in a microcentrifuge tube. The final step involved purifying the double-stranded cDNA. This was achieved by mixing several solutions and subjecting the sample to repeated centrifugation steps to separate the supernatant and pellet. The cDNA pellet was subsequently combined with TE buffer and stored at -20 °C for further use in downstream applications.

Real-Time Polymerase Chain Reaction (RT-PCR)

Real-time PCR was performed using a two-step system (Genechecker UF-300) and the Sensifast cDNA Synthesis protocol (Meridian Bioscience). Gene expression was analyzed in duplicate for each sample. A master mix was prepared, and 10 µL was dispensed into each well of the PCR chip. The PCR program consisted of an initial denaturation step at 95 °C for 60 s, followed by 40 cycles of denaturation at 95 °C for 15 s, annealing at 60 °C for 15 s, and extension at 72 °C for 45 s.

Data Analysis

Real-time PCR data were analyzed using the $2^{-\Delta\Delta CT}$ (Livak) method to quantify relative gene expression levels from obtained cycle threshold (CT) values. These relative expression values were then graphically presented. One-way ANOVA was used for statistical analysis, with a significance level set at 95% confidence ($p < 0.05$). If significant differences were found, Tukey's post-hoc test was applied. The effect of deferasirox was determined by observing the reduction in target gene expression levels among the treatment groups.

Results and Discussion

Expression of *Fth1* in the Spleen Organ

Gene expression analysis showed a 2.26-fold increase in *Fth1* gene expression in the iron dextran group (KN) when compared to the normal group (N) (see **Figure 1**). This indicates that iron overload in the KN group rats significantly ($p < 0.05$) elevated *Fth1* gene expression relative to the standard control. Conversely, the deferasirox treatment group (KP), which received deferasirox, exhibited a 3.28-fold decrease in *Fth1* gene expression compared to the negative control. Although statistically insignificant, this trend suggests that deferasirox administration in iron-overloaded rats might decrease *Fth1* gene expression.

The regulation of ferritin protein levels occurs primarily at the post-transcriptional level and is influenced by the cellular iron status via iron-responsive elements (IREs) located on ferritin mRNA (25). This mechanism enables increased ferritin expression during iron overload and decreased expression when iron levels are depleted. This post-

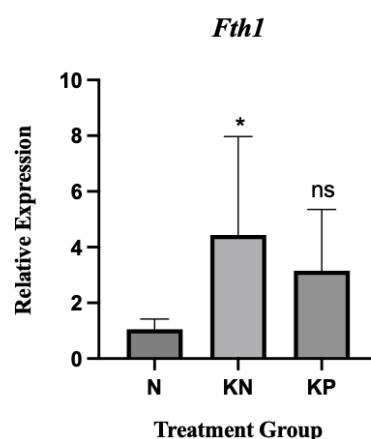


Figure 1. Relative expression of *Fth1* in the normal/healthy control group (N), negative control group (KN; iron dextran-induced, untreated), and deferasirox-treated group (KP). ns indicates a non-significant difference; (*, $p < 0.05$) indicates a significant difference compared to group N.

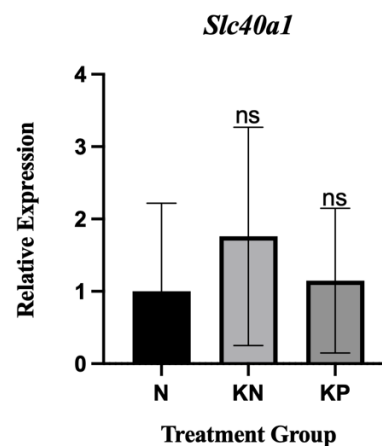


Figure 2. Relative expression of *Slc40a1* in the normal/healthy control group (N), negative control group (KN; iron dextran-induced, untreated), and deferasirox-treated group (KP). Note: ns indicates a non-significant difference.

transcriptional control likely explains the reduction in *Fth1* expression observed after administration of an iron chelator. Iron chelators, particularly deferasirox, function by binding excess ferric iron in the body, forming stable ferric complexes that are then excreted through feces (26). The reduction in iron levels caused by deferasirox prevents iron regulatory proteins (IRPs) from binding to iron; instead, IRPs bind to the IRE at the 5' end of *Fth1* mRNA. This IRP-IRE binding impedes ribosomal access, thereby inhibiting mRNA translation (27). The lack of statistical significance in the treatment group may be due to the spleen's relatively slow response to iron chelation, particularly since deferasirox is more effective in targeting cardiac iron (28).

Expression of *Slc40a1* in the Spleen Organ

Figure 2 illustrates the average relative gene expression across each treatment group. Quantitative analysis revealed a 1.72-fold increase in *Slc40a1* gene expression in the iron dextran (KN) group compared to the normal (N) group. This elevated expression subsequently decreased in the deferasirox treatment group (KP), indicating that deferasirox administration may influence *Slc40a1* expression, resulting

in a 1.15-fold reduction, although the change was not statistically significant ($p > 0.05$).

The regulation of ferroportin in the body is complex and responsive to various physiological conditions and pathological states. Under conditions of iron overload, ferroportin protein levels are typically reduced relative to normal conditions. This suppression serves to prevent systemic iron dissemination by retaining iron within overloaded tissues or organs (29). The decrease in ferroportin levels is primarily attributed to elevated hepcidin, which binds to and induces the internalization and degradation of ferroportin (30). Interestingly, in contrast to ferroportin protein levels, *Slc40a1* mRNA expression in the spleen increased under iron-overload conditions. This apparent discrepancy may be explained by the regulation of *Spi-C* and *Bach1* transcription factors in red pulp macrophages (31). *Spi-C* is essential for the development of red pulp macrophages (32), but under normal conditions, its activity is repressed by *Bach1* (33). During iron overload, heme accumulation from increased red blood cell degradation leads to *Bach1* degradation, thereby lifting its inhibitory effect on *Spi-C* (34). As a result, *Nrf2* is activated and *Spi-C* activity increases, promoting monocyte differentiation into macrophages that express ferroportin and heme oxygenase-1 through enhanced transcription of both genes (35). The irregular, non-significant increase and decrease in *Slc40a1* expression observed in the spleen, as shown in **Figure 2**, deviates from expected regulatory patterns. This may be due to inflammatory responses experienced by the rats, potentially disrupting the hepcidin-ferroportin regulatory axis (36). Alternatively, the dose or duration of iron dextran administration may have been insufficient to elicit a strong regulatory response in the spleen. Further studies with a larger sample size and higher iron dextran dosage are warranted to confirm this hypothesis.

Expression of *Hmox1* in the Spleen Organ

Based on the statistical results of *Hmox1* expression, it can be concluded that there were highly significant differences ($p < 0.05$) in relative gene expression among the three treatment groups. This significance is further illustrated in **Figure 3**, where asterisks (*) denote statistical differences; a greater number of asterisks between group comparisons indicates a larger magnitude of expression difference. Calculations using the Livak method revealed an increasing trend in relative *Hmox1* expression across the treatment groups. The iron dextran group (KN) exhibited a significantly higher expression compared to the control group (N), with a 24.29-fold increase. Unexpectedly, deferasirox administration in the KP group resulted in a 55.25-fold increase in iron absorption. Further research with a larger sample size and additional supporting tests is needed to confirm the underlying cause of this observation.

The pronounced increase in *Hmox1* expression following deferasirox administration warrants further investigation due to several potential contributing factors. These include the presence of active compounds within deferasirox or intrinsic physiological mechanisms that trigger red pulp macrophages to upregulate *Hmox1* expression despite reduced iron levels (37). Another possibility is that deferasirox targets iron stores more effectively in organs other than the liver (38). Moreover, deferasirox typically requires a prolonged period, at least three months or more, to exert its antioxidant effects (39). In some studies, deferasirox has also been shown to

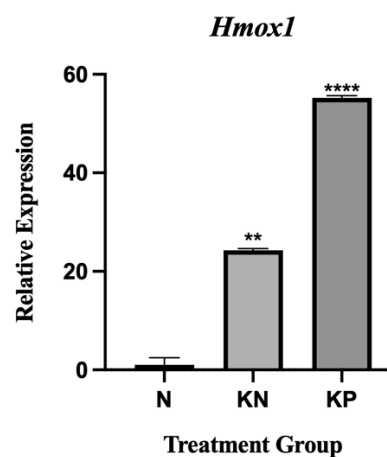


Figure 3. Relative expression of *Hmox1* in the normal/healthy control group (N), negative control group (KN; iron dextran-induced, untreated), and deferasirox-treated group (KP). Significance: (**, $p < 0.01$) vs. N; (****, $p < 0.001$) vs. N and KN.

increase the expression of nuclear factor erythroid 2-related factor 2 (*Nrf2*) (40), a key transcription factor involved in regulating numerous iron-related genes, particularly under conditions of oxidative stress (41). The upregulation of *Nrf2* may significantly contribute to the induction of *Hmox1* expression in the deferasirox-treated (KP) rats, thereby explaining the observed surge in *Hmox1* levels following chelator administration (42).

Conclusion

Based on the findings of this study, it can be concluded that the iron-regulatory genes *Fth1*, *Slc40a1*, and *Hmox1* are constitutively expressed under physiological conditions, with significant upregulation observed during states of iron overload. This expression pattern suggests their active involvement in maintaining iron homeostasis. While deferasirox administration did not significantly reduce *Fth1* and *Slc40a1* expression, it markedly increased *Hmox1* levels, indicating a selective gene response to iron chelation. The pronounced upregulation of *Hmox1* may reflect an adaptive mechanism to counteract oxidative stress triggered by iron accumulation, underscoring its dual role in iron detoxification and cellular protection. These findings highlight the differential regulatory pathways engaged by each gene and provide insights into how iron chelation therapy might influence both iron metabolism and oxidative stress responses at the molecular level.

Declarations

Author Informations

Annisa Maharani Wibowo

Affiliation: Department of Biology, Faculty of Mathematics and Natural Sciences, Universitas Padjadjaran, Jatinangor 45363, West Java, Indonesia.

Contribution: Conceptualization, Data Curation, Formal analysis, Investigation, Methodology, Validation, Visualization, Writing - Original Draft, Writing - Review & Editing.

Yasmi Purnamasari Kuntana

Affiliation: Department of Biology, Faculty of Mathematics and Natural Sciences, Universitas Padjadjaran, Jatinangor

45363, West Java, Indonesia.

Contribution: Data Curation, Investigation, Methodology, Validation, Writing - Review & Editing.

Tanendri Arrizqiani

Affiliation: Department of Biology, Faculty of Mathematics and Natural Sciences, Universitas Padjadjaran, Jatinangor 45363, West Java, Indonesia.

Contribution: Formal analysis, Software, Visualization, Writing - Review & Editing.

Ratu Safitri

Corresponding Author

Affiliation: Department of Biology, Faculty of Mathematics and Natural Sciences, Universitas Padjadjaran, Jatinangor 45363, West Java, Indonesia.

Contribution: Conceptualization, Funding acquisition, Project administration, Resources, Supervision, Writing - Review & Editing.

Conflict of Interest

The authors declare no conflicting interest.

Data Availability

The unpublished data is available upon request to the corresponding author.

Ethics Statement

This research received ethical approval from the Animal Research Ethics Committee of Universitas Padjadjaran, Bandung, under approval number 75/UN6.KEP/EC/2023. All procedures involving experimental animals were conducted in strict accordance with the ethical guidelines established by Universitas Padjadjaran, based on internationally accepted principles for the humane treatment of animals.

Funding Information

The author(s) declare that no financial support was received for the research, authorship, and/or publication of this article.

References

- Ahmed OM, Mustafa TM. Oxidative Stress: The Role of Reactive Oxygen Species (ROS) and Antioxidants in Human Diseases. *Plant Archives*. 2020;20(2):4089-4095.
- Wang X, Ye L, Li H, Jie L, Cun L, Changgang S. Role of Flavonoid in The Treatment of Iron Overload. *Frontiers in Cell and Developmental Biology*. 2021;9(1):1-12.
- Jobanputra M, Clark P, Sandra GL, Michael M, Paul T. Co-Morbidities and Mortality Associated with Transfusion-Dependent Beta-Thalassemia in Patients in England: A 10 Year Retrospective Cohort Analysis. *British Journal of Haematology*. 2020;191(5):897-905.
- Fianza PI, Anita R, Sri HW, Shofura A, Ghozali M, Andre I, Dilli MAP, Dimmy P, Teddy AS, Mas RAAAS, Djatnika S, Suthat F, Ramdan P. Iron Overload in Transfusion-Dependent Indonesian Thalassemic Patient. *Anemia*. 2021;1(1):1-8.
- Yiannikourides A, Gladys OL. A Short Review of Iron Metabolism and Pathophysiology of Iron Disorders. *Medicines*. 2019;6(3):85-92.
- Lewis SM, Adam W, Stephanie CE. Structure and Function of The Immune System in The Spleen. *Science Immunology*. 2019;4(33):1-13.
- Recalcati S. & Gaetano C. Macrophages and iron: a special relationship. *Biomedicines*. 2021;9(11):1585.
- Vogt ACS, Tasneem A, Mona M, Monique V, Vania M, Martin FB. On Iron Metabolism and Its Regulation. *International Journal of Molecular Science*. 2021;22(9):4591.
- Xiong X, Li W, Yu C, Qiu M, Zhang Z, Hu C, Zhu S, Yang L, Pen H, Song X, Chen J, Xia B, Han S, Yang C. SMURF1-induced ubiquitination of FTH1 disrupts iron homeostasis and suppresses myogenesis. *Int J Mol Sci*. 2023;26(3):1390.
- Xie Q, Wang J, Li R, Liu H, Zhong Y, Xu Q, Ge Y, Li C, Sun L, Zhu J. IL-6 signaling accelerates iron overload by upregulating DMT1 in endothelial cells to promote aortic dissection. *Int J Biol Sci*. 2024;20(11):4222-4227.
- Berezovsky B, Frýdlová J, Gurieva I, Rogalsky DW, Vokurka M, Krijt J. Heart ferroportin protein content is regulated by heart iron concentration and systemic hepcidin expression. *Int J Mol Sci*. 2022;23(11):5899.
- Hamad M, Mohammed AK, Hachim MY, Mukhopadhy D, Khalique A, Laham A, Dhaiban S, Bajbouj K, Taneera J. Heme oxygenase-1 (HMOX-1) and inhibitor of differentiation proteins (ID1, ID3) are key response mechanisms against iron-overload in pancreatic β -cells. *Mol Cell Endocrinol*. 2021;538:111462.
- Sebastián VP, Salazar GA, Coronado-Arrázola I, Schultz BM, Vallejos OP, Berkowitz L, Álvarez-Lobos MM, Riedel CA, Kalergis AM, Bueno SM. Heme oxygenase-1 as a modulator of intestinal inflammation development and progression. *Front Immunol*. 2018;9:1956.
- Aydinok Y. Iron chelation therapy as a modality of management. *Hematol Oncol Clin North Am*. 2018 Apr;32(2):261-275.
- Salimi Z, Afsharinasab M, Rostami M, Eshaghi Milasi Y, Mousavi Ezmareh SF, Sakhaei F, Mohammad Sadeghipour M, Rasooli Manesh SM, Asemi Z. Iron chelators: as therapeutic agents in diseases. *Ann Med Surg (Lond)*. 2024 Mar 19;86(5):2759-2776.
- Arfie NG, Bambang SZ, Sudarmanto. Efektivitas dari Deferasirox pada Pasien Thalassemia Mayor: Article Review. *Jurnal Sains dan Kesehatan*. 2022;4(3):354-362.
- Rahdar A, Reza HM, Saman S, Bilal M, Barani M, Pouya K, George ZK. Biochemical Effects of Deferasirox and Deferasirox-Loaded Nanomicelles in Iron-Intoxicated Rats. *Life Science*. 2021;270(1):25-34.
- Honari N, Sayadi M, Sajjadi SM, Solhjoo S, Anani Sarab G. Deferasirox improved iron homeostasis and hematopoiesis in ovariectomized rats with iron accumulation. *Sci Rep*. 2025;15:2449.
- Shaker RA, Rizij FA, Jasim TA. Deferasirox adherence in patients with thalassemia: Exploring the association with patient knowledge and ferritin levels. *Pharmacia*. 2024;71:1-6.
- Arifin WN, Zahiruddin WM. Sample Size Calculation in Animal Studies Using Resource Equation Approach. *Malays J Med Sci*. 2017;24(5):101-105.
- Badan Pengawas Obat dan Makanan. Pedoman Uji Farmakodinamik Pratiklinik Obat Tradisional. Jakarta: Badan Pengawas Obat dan Makanan; 2021. Available from: <https://jdih.pom.go.id/download/fiip/1282/18/2021>
- Zhang H, Pavel Z, Shaohua W, Gavin YO. Role of Iron Metabolism in Heart Failure: From Iron Deficiency to Iron Overload. *Biochimica et Biophysica Acta-Molecular Basis of Disease*. 2019;1865(7):1925-1937.
- Arrizqiyani T, Syamsunarno MRAA, Safitri R. Molecular mechanism of sappen wood extract in rat liver and kidney models with iron overload. *Adv Anim Vet Sci*. 2025;13(4):883-891.
- Shukla SK, Shrivastava A, Mishra PC. Effect of deferasirox on serum ferritin level in children with thalassemia major: impact of transfusional iron load. *Int J Contemp Pediatr*. 2019;6(5):2081-2086.
- Purnomo VV, Sareh AT, Risma. Manalagi Apple Vinegar (*Malus sylvestris* Mill) as Anti Diabetic to Alloxan Induced Wistar White Male Rate. *Oceana Biomedicina Journal*. 2019;2(1):44-51.
- Daru J, Katherine C, Simon JS, Barbara De La S, Erica MW, Sant-Rayn P. Serum Ferritin as an Indicator of Iron Status: What Do We Need to Know? *The American Journal of Clinical Nutrition*. 2017;106(6):1634-1639.
- Wei Y, Xiaoxiao S, Ying G, Yonghong G, Yuanyuan L, Lian G. Iron Toxicity in Intracerebral Hemorrhage: Physiopathological and Therapeutic Implications. *Brain Research Bulletin*. 2022;178(1):144-154.
- Nick H, Allegrini PR, Fozard L, Junker U, Rojkjaer L, Salie R,

- Niederkofler V, O'Reilly T. Deferasirox reduces iron overload in a murine model of juvenile hemochromatosis. *Exp Biol Med* (Maywood). 2009 May;234(5):492-503.
29. Yanatori I, Des RR, Herschel SD, Shinya T, Fumio K. CD63 is Regulated by Iron via The IRE-IRP System and is Important for Ferritin Secretion by Extracellular Vesicles. *Blood*. 2018;138(16):1490-1503.
30. Drakesmith H, Nemeth E, Ganz T. Ironing out Ferroportin. *Cell Metab*. 2015;22(5):777-787.
31. Pantopoulos K. Inherited disorders of iron overload. *Front Nutr*. 2018;5:103.
32. Srinoun K, Svasti S, Chumworathayee W, Winichagoon P. BACH1 regulates erythrophagocytosis and iron-recycling in β -thalassemia. *Genes Cells*. 2022;28(6):366570464.
33. Kohyama M, Ise W, Taguchi H, Nakano H, Abe T, Okazaki T, et al. Role for Spi-C in the development of red pulp macrophages and splenic iron homeostasis. *Nature*. 2009 Jan 15;457(7227):318-321.
34. Haldar M, Freeburne J, Arndt C, Sheng S, Bowdridge S, Eisenstein RS, et al. Heme-mediated SPI-C induction promotes monocyte differentiation into iron-recycling macrophages. *Elife*. 2014;3:e01750.
35. Ricci A, Giada Di B, Elisa B, Elena B, Elena C, Paolo V. Iron Metabolism in The Disorders of Heme Biosynthesis. *Metabolites*. 2022;12(9):819.
36. Liu XB, Nguyen NB, Marquess KD, Yang F, Haile DJ. Regulation of hepcidin and ferroportin expression by lipopolysaccharide in splenic macrophages. *Blood Cells Mol Dis*. 2005 Jul-Aug;35(1):47-56.
37. Haldar M, Freeburne J, Arndt C, Sheng S, Bowdridge S, Eisenstein RS, et al. Heme-mediated SPI-C induction promotes monocyte differentiation into iron-recycling macrophages. *Elife*. 2014;3:e01750.
38. Oliveira J de, Beraldo DM, Cardoso DL. Crosstalk between Heme-Oxygenase-1 and Iron Metabolism in Macrophages: Implications for the Modulation of Inflammation and Immunity. *Antioxidants*. 2022;11(5):861.
39. Talebi Y, Shahverdi S, Tabibian S. Comparison of iron chelation effects of deferoxamine, deferasirox, and combination of deferoxamine and deferiprone on liver and cardiac T2 MRI in thalassemia major. *J Res Pharm Pract*. 2017;6(3):149-154.
40. Saigo K, Kono M, Takagi Y, Takenokuchi M, Hiramatsu Y, Tada H, Hishita T, Misawa M, Imoto S, Imashuku S. Deferasirox reduces oxidative stress in patients with transfusion dependency. *J Clin Med Res*. 2013;5(1):57-60.
41. Hsu WY, Wang LT, Lin PC, Liao YM, Hsu SH, Chiou SS. Deferasirox Causes Leukaemia Cell Death through Nrf2-Induced Ferroptosis. *Antioxidants (Basel)*. 2024 Mar 29;13(4):451.
42. Jia D, Cai Z, Zeng H. Nrf2 activators for the treatment of rare iron overload diseases: From bench to bedside. *J Adv Res*. 2025;69:11876910.

Additional Information


How to Cite

Annisa Maharani Wibowo, Yasmi Purnamasari Kuntana, Tanendri Arrizqiani, Ratu Safitri. Differential Regulation of *Slc40a1*, *Fth1*, and *Hmx1* by Deferasirox in Splenic Iron Overload. *Sciences of Pharmacy*. 2025;4(4):286-291

Publisher's Note

All claims expressed in this article are solely those of the authors and do not necessarily reflect the views of the publisher, the editors, or the reviewers. Any product that may be evaluated in this article, or claim made by its manufacturer, is not guaranteed or endorsed by the publisher. The publisher remains neutral with regard to jurisdictional claims in published maps and institutional affiliations.

Open Access

 This article is licensed under a Creative Commons Attribution 4.0 International License. You may share and adapt the material with proper credit to the original author(s) and source, include a link to the license, and indicate if changes were made.